THE JOURNAL OF BIOLOGICAL CHEMISTRY VOL. 284, NO. 51, pp. 35702–35713, December 18, 2009

Early Transcriptional Arrest at *Escherichia coli rplN* and *ompX* Promoters*[S]

Received for publication, August 9, 2009, and in revised form, October 15, 2009 Published, JBC Papers in Press, October 23, 2009, DOI 10.1074/jbc.M109.053983

Ekaterina Stepanova[‡§], **Minshi Wang**[‡], **Konstantin Severinov**[§¶‖], **and Sergei Borukhov**[‡1]

From the [‡]*Department of Cell Biology, School of Osteopathic Medicine at Stratford, University of Medicine and Dentistry of New Jersey, Stratford, New Jersey 08084, the* [¶]*Waksman Institute, Rutgers University, Piscataway, New Jersey 08854, the* [§]*Institute of Biology of Gene, Russian Academy of Sciences, Moscow 119334, Russia, and the* [‖]*Institute of Molecular Genetics, Russian Academy of Sciences, Moscow 123182, Russia*

Bacterial transcription elongation factors GreA and GreB stimulate the intrinsic RNase activity of RNA polymerase (RNAP), thus helping the enzyme to read through pausing and arresting sites on DNA. Gre factors also accelerate RNAP transition from initiation to elongation. Here, we characterized the molecular mechanism by which Gre factors facilitate transcription at two *Escherichia coli* promoters, P*rplN* and P*ompX*, that require GreA for optimal *in vivo* activity. Using *in vitro* transcription assays, $KMnO_4$ footprinting, and Fe^{2+}-induced hydroxyl radical mapping, we show that during transcription initiation at P*rplN* and P*ompX* in the absence of Gre factors, RNAP falls into a condition of promoter-proximal transcriptional arrest that prevents production of full-length transcripts both *in vitro* and *in vivo*. Arrest occurs when RNAP synthesizes 9–14-nucleotide-long transcripts and backtracks by 5–7 (P*rplN*) or 2–4 (P*ompX*) nucleotides. Initiation factor σ^{70} contributes to the formation of arrested complexes at both promoters. The signal for promoter-proximal arrest at P*rplN* is bipartite and requires two elements: the extended −10 promoter element and the initial transcribed region from positions +2 to +6. GreA and GreB prevent arrest at P*rplN* and P*ompX* by inducing cleavage of the 3′-proximal backtracked portion of RNA at the onset of arrested complex formation and stimulate productive transcription by allowing RNAP to elongate the 5′-proximal transcript cleavage products in the presence of substrates. We propose that promoter-proximal arrest is a common feature of many bacterial promoters and may represent an important physiological target of regulation by transcript cleavage factors.

Transcript cleavage factors such as Gre factors in bacteria and the SII factor in eukaryotes are ubiquitous in nature, but their physiological role(s) is poorly understood. Transcript cleavage factors stimulate RNA polymerase (RNAP)[2] intrinsic nucleolytic activity, an evolutionarily conserved function of all multisubunit RNAPs (reviewed in Refs. 1 and 2). *In vitro*, Gre/SII factors suppress or prevent transcription pausing and transcription arrest during elongation (3, 4), enhance transcription fidelity (5, 6), facilitate promoter escape by RNAP (7–9), and assist in transcription-coupled DNA repair (10). During transcription *in vitro* and *in vivo*, RNAP can become arrested upon encountering a roadblock such as a DNA-binding protein or a special DNA sequence (1, 11). Some roadblocks induce RNAP to slide backwards along the template ("backtrack") (11–14), forcing the nascent RNA 3′-terminus to extrude through the RNAP secondary channel, typically by 2–18 nt (1–4, 12, 13). Endonucleolytic cleavage of such extruded RNA by the RNAP catalytic center generates a new 3′ terminus that can be extended in the presence of rNTPs, giving RNAP another chance to read through the roadblock (11–14). RNA cleavage by RNAP alone is inefficient under physiological conditions but is markedly stimulated by Gre/SII or, in the absence of the factors, by alkaline pH or pyrophosphate (15–17).

Transcript cleavage factors contribute to transcription proofreading *in vitro* because incorporation into nascent RNA of nucleotide analogs that disrupt the RNA-DNA hybrid induces backtracking, generating transcription complexes that are subject to Gre-induced RNA hydrolysis (12, 18, 19). The cleavage activity of Gre factors is also part of the cellular mechanism that resolves conflicts between transcription and the processes of DNA repair/replication. Gre factors help remove stalled or backed up RNAPs from sites of chromosomal lesions caused by UV irradiation or chemicals and thus provide access of DNA repair/recombination apparatus to the lesion sites (20). Gre factors also help resolve collisions between replication forks and RNAP stalled at transcription terminators during co-directional replication and transcription (21).

The transition from transcription initiation to transcription elongation is also facilitated by Gre-induced transcript cleavage (7, 9). Gre factors dramatically reduce the amounts of abortive products, both *in vitro* and *in vivo* (7, 9, 22–24), and induce substantial cleavage of abortive transcripts (7, 22). Recent studies suggested that DNA may undergo "scrunching" during

* This work was supported, in whole or in part, by National Institutes of Health Grants GM54098 (to S. B.) and GM59295 (to K. S.), by University of Medicine and Dentistry of New Jersey Research Foundation (to S. B.), and by the Molecular and Cell Biology Program Grant of the Presidium of Russian Academy of Sciences (to K. S.).

[S] The on-line version of this article (available at http://www.jbc.org) contains supplemental Figs. S1–S3.

[1] To whom correspondence should be addressed: Dept. of Cell Biology, UMDNJ-SOM at Stratford, 2 Medical Center Dr., Rm. 108b, Stratford, NJ 08084-1489. Tel.: 856-566-6271; Fax: 856-566-6965; E-mail: s.borukhov@umdnj.edu.

[2] The abbreviations used are: RNAP, RNA polymerase; nt, nucleotide(s); wt, wild type; TB, transcription buffer; SB, sample buffer; TC, transcription complex.

abortive initiation, which could account for long (>9 nt) abortive products synthesized by RNAP at some promoters. Stress accumulated during scrunching (25, 26) is thought to be relieved either through disruption of RNAP-promoter contacts, leading to RNAP escape from promoter or, through a reversal of scrunching, to dissociation of the abortive transcript through the RNAP secondary channel. While inducing endonucleolytic cleavage of abortive transcripts, Gre factors are thought to simultaneously prevent the 5′-terminal RNA fragment from dissociating, thus increasing the fraction of RNAP bound to nascent RNA and stimulating promoter escape (7, 24, 27).

Previous microarray studies identified 31 *Escherichia coli* operons that are up-regulated by GreA *in vivo* (23). *In vitro* analysis of 10 randomly selected promoters that controlled genes whose expression was increased by GreA revealed that the factor stimulated *E. coli* RNAP transcription from these promoters at the stage of transcription initiation and/or promoter escape (23). The exact mechanism of Gre-induced transcription stimulation was not defined. To reveal this mechanism, we chose two promoters previously shown to be stimulated by GreA *in vivo* and *in vitro*: the outer membrane protein gene *ompX* promoter P*ompX* and ribosomal proteins operon *rplN-rpmJ* promoter P*rplN*, and characterized in detail *in vitro* transcription products formed on these promoters, both in the presence and in the absence of transcript cleavage factors. Our data show that on these promoters and, by extension, on other Gre-dependent promoters, a novel type of transcription complex, a promoter-proximal arrested complex, is formed with high efficiency in the absence of Gre factors. Initiation factor σ contributes to formation of promoter-proximal arrested complexes at both promoters studied. At least in the case of P*rplN*, the signal for promoter-proximal transcriptional arrest is bipartite and requires the presence of elements upstream and downstream of the transcription start site. Because RNAP is unable to escape from promoter-proximal arrested complexes, their formation leads to occlusion of the initial transcribed sequence of the promoter and, ultimately, to cessation of productive transcription. Through their transcript cleavage activity, Gre factors either rescue promoter-proximal arrested complexes or prevent their formation, thus allowing efficient transcription and gene expression. Our analysis, along with the previous transcript profiling data, suggests that rescue of promoter-proximal arrested complexes may be one of the main physiological function of Gre factors.

EXPERIMENTAL PROCEDURES

Strains, Plasmids, and Proteins

The wild type (wt) *E. coli* RNAP was purified from *greA*$^-$/*greB*$^-$ *E. coli* strain BW32645 (*rrnB3* Δ*lacZ4787 hsdR514* Δ(*araBAD*)*567* Δ(*rhaBAD*)*56* Δ*greA* Δ*greB*) (23) by standard procedures (15). RNAP carrying His_6 tag at the C terminus of the β′ subunit was purified from the *greA*$^-$/*greB*$^-$ *E. coli* strain BW32645 transformed with pCYB2β′C-PKA (28). Mutant σ-L402F, was purified as described (29) using expression plasmid pHTσL402F (generously provided by J. W. Roberts). *E. coli* His_6-tagged wt GreA, GreB, and mutant GreA-D41E were overexpressed and purified as described (28).

Plasmids pES-rplN, and pES-ompX were derivatives of pRLG862 (30) where the sequence of rrnB P1 promoter [−88; +150] was replaced using HindIII and EcoRI by sequences of P*rplN* [−72;+160] and P*ompX* [−175; +129] promoter fragments, respectively, followed by terminator T1.

Reporter plasmids prplN-lacZ and pompX-lacZ were derivatives of pBAD/Myc-His/LacZ (Invitrogen) with the following modifications. The original pBAD/Myc-His/LacZ vector carrying ColEI origin of replication and ampicillin resistance marker was digested with SphI and NcoI to remove *araC* and P*araBAD* promoter. The resulting 5923-bp fragment was gel-purified and ligated with SphI-NcoI PCR fragment containing P*rplN* [−72; +46] followed by XbaI site and ~30 bp-long sequence of Shine-Dalgarno element from the phage φX174 gene E (used to decrease toxicity of LacZ expression under strong P*rplN* (31), yielding prplN-lacZ. The pompX-lacZ was obtained by replacing the SphI-XbaI P*rplN* fragment in prplN-lacZ with a SphI-XbaI PCR fragment containing P*ompX* [−175; +129]. Gre expression plasmids (pBAD-GreAwt and pBAD-GreA-D41E) compatible with reporter plasmids described above were constructed using pBAD33 vector (Invitrogen) carrying the P15 origin of replication and spectinomycin resistance. Expression of wt and mutant GreA was under the control of arabinose-inducible P*ara* promoter. The sequences of primers used for construction of PCR amplification and cloning of P*rplN* and P*ompX* DNA fragments into reporter plasmids and of wt *greA* and *greA-D41E* genes into compatible expression vectors are available upon request.

The wt P*rplN* [−84; +45] and P*T7A1* [−148; +77], the mutant P*rplN* [−84; +46] or [−84; +77], and the hybrid, P*rplN/T7A1* [−84; +50] and P*T7A1/rplN* [−148; +46] promoter variants were constructed by PCR using appropriate upstream and downstream primers (sequences are available upon request) to generate shortened promoter DNA templates (see Fig. 6 for details).

In Vitro Transcription Reactions

Run-off Transcription Assays—DNA fragments used for *in vitro* transcription assays were generated by PCR using appropriate primers resulting in 161-bp-long PrplN [−84;+77] and 236-bp-long PompX [−188;+65] DNA templates. Multiround transcription reactions were carried out in 10 μl of transcription buffer (TB; 40 mM Tris-HCl, pH 7.2, 10 mM $MgCl_2$, 70 mM KCl, 0.1 mM dithiothreitol, 0.1 mg/ml bovine serum albumin) containing 100 μM NTPs, 0.165 μM [α-P^{32}]ATP (3000 Ci/mmol), 0.1 pmol of DNA template, 0.3 pmol of *E. coli* RNAP core, and 1 pmol of σ factor (wt σ or σL402F) in the presence or absence of 4 μM GreA or 0.4 μM GreB. Single-round reactions were performed as above but in the presence of 10 μg/ml rifampicin (32). After incubation for 15 min at 37 C, all of the reactions were stopped by 10 μl of formamide sample buffer (SB; 50 mM EDTA in 90% formamide), and the RNA products were separated by denaturing 23% (21:3) PAGE, containing 8 M urea, and quantified by Typhoon PhosphorImager (GE Healthcare) using ImageQuant (Molecular Dynamics).

Preparation, Transcript Cleavage, and RNA Extension Assays of Inactive Stalled (Arrested) Promoter-proximal Complexes—TCs arrested at P*rplN* were prepared in solution by incubation of 1.5 pmol of linear DNA template [−84;+77] with 3 pmol of RNAP holoenzyme in 30 μl of TB containing 30 μM NTPs, 0.1 μM [γ-P^{32}]GTP (4500 Ci/mmol) in the absence of Gre factors for 10 min at 37 C. The reaction mixture was applied on G-50 Quick-Spin gel filtration columns to remove NTPs and abortive RNA. For transcript cleavage and NTP-chase experiments, a 4-μl aliquot of purified arrested TCs was incubated in 10 μl of TB alone or together with 4 μM GreA, (or 0.4 μM GreB) in the absence or presence of 100 μM NTPs for 10 min at 37 °C (see Fig. 1*A*). The reactions were terminated by the addition of SB and analyzed as described above.

TCs arrested at P*ompX* were prepared using 10 μl of nickel-nitrilotriacetic acid-agarose beads carrying 10 pmol of immobilized His-tagged RNAP holoenzyme in 120 μl of TB containing 30 μM NTPs, 0.165 μM [α-P^{32}]ATP (3000 Ci/mmol), and 3 pmol of template DNA [−188;+65]. After incubation for 15 min at 37 °C, a 10-μl aliquot was withdrawn, and the reaction was stopped with SB. The remaining 110 μl of bead suspension were washed with 3 × 1 ml of TB to remove NTPs and abortive RNA products, and the suspension was divided into three portions and treated with TB alone, 4 μM GreA, or 0.4 μM GreB. After incubation for 5 min at 37 °C, 10-μl aliquots were withdrawn, and the reactions were terminated by SB. The remaining beads were washed again with 3 × 1 ml of TB to remove dissociated 3′-terminal RNA cleavage products, and the cleaved TCs were chased with 100 μM NTPs (see Fig. 1*B*).

DNA Footprinting and RNA Mapping

Localized Fe^{2+}-mediated Hydroxyl Radical Mapping—Mapping of the position of the catalytic center in promoter-proximal arrested TCs at P*rplN*, by localized Fe^{2+}-mediated hydroxyl radical cleavages was performed as described (12). Arrested TCs were prepared under same conditions as described above, purified by Quick-Spin Sephadex G-50 (see Fig. 1*A*), and equilibrated in chelated TB without Mg^{2+}. Hydroxyl-radical RNA cleavage reactions were carried out by incubation of arrested TCs in 10 μl of hydroxyl cleavage buffer (20 mM Na-HEPES, pH 7.5, 150 mM NaCl, 0.1 mg/ml bovine serum albumin) containing 0.1 mM $(NH_4)_2Fe(SO_4)_2$ and 1 mM dithiothreitol for 20 min at 30 °C. In control reactions, arrested TCs were incubated as above but in the presence of 10 mM $MgCl_2$ or 50 mM EDTA (see Fig. 2). The reaction was stopped by the addition of 3 volumes of 7 mM thiourea solution and washed by chloroform, and the RNA products were precipitated by ethanol, dissolved in SB, and resolved on denaturing 23% PAGE.

In Vitro DNA Footprinting by $KMnO_4$—Binary and ternary transcription complexes formed on PrplN and PompX were probed with $KMnO_4$ as described (33). 1 μl of *10 m*M KMnO4 was added to 10 μl of transcription complex. After incubation for 40 s, the reaction was stopped with 1.5 μl of β-mercaptoethanol followed by chloroform extraction and DNA precipitation by ethanol. The resulting DNA was dissolved in 10 μl of 10 mM Tris-HCl, pH 7.5, and used as a template for primer extension reaction using radiolabeled primers (same as those used for PCR and cloning of PrplN and PompX into pES-rplN or pES-ompX) in 10 linear PCR cycles. The reaction was stopped by SB, and the modified thymidines were visualized by 6% sequencing PAGE.

$KMnO_4$ Reactivity in Vivo—The reactivity of plasmid DNAs carrying PrplN and PompX to $KMnO_4$ *in vivo* was determined essentially as described (29). The reactions were conducted in the *E. coli greA*$^-$*/greB*$^-$ strain BW32645 or the isogenic *greA*$^+$*greB*$^-$ strain BW32613 (23) carrying reporter plasmid pES-rplN or pES-ompX. The cells were grown in 9 ml of LB medium to A_{600} = 0.5, then 1 ml of 100 mM $KMnO_4$ was added, and the cells were shaken for 3 min at 37 °C. The treated cells were pelleted, placed on ice, resuspended in 300 μl of STET buffer (50 mM Tris-HCl, pH 8.0, 50 mM EDTA, 8% sucrose, 5% Triton X-100) containing 200 μg of lysozyme. After 10 min of incubation, the cell suspensions were heated at 95 °C for 2 min and centrifuged for 10 min. The supernatants were treated with RNase A, and the modified pDNA was purified by QIAquick spin columns (Qiagen; QIAquick nucleotide removal kit). For pDNA quantity normalization in all samples, dot blot hybridization was carried out along with ethidium bromide staining of linearized pDNA after agarose gel electrophoresis. The modified thymidines were detected by primer extension reactions using radiolabeled primers (same as those used for PCR and cloning of PrplN and PompX into pES-rplN or pES-ompX) and analyzed by 6% sequencing PAGE as above.

β-Galactosidase Assay—For measurements of β-galactosidase activity, cultures of *E. coli greA*$^-$*/greB*$^-$ strain BW32645 co-transformed with reporter plasmid prplN-lacZ or pompX-lacZ together with Gre expression plasmids pBAD-GreAwt or pBAD-GreA-D41E or control vector pBAD33 were grown in LB to A_{600} = 0.5. 100 μl of cell culture were centrifuged and resuspended in 100 μl of permeabilization solution (100 mM Na_2HPO_4, 20 mM KCl, 2 mM $MgSO_4$, 0.8 mg/ml hexadecyltrimethyl-ammonium bromide, 0.4 mg/ml sodium deoxycholate, 5.4 μl/ml β-mercaptoethanol) containing 100 μg/ml of chloramphenicol (to terminate translation). After 30 min of incubation at 37 °C, 300 μl of prewarmed substrate solution (60 mM Na_2HPO_4, 40 mM NaH_2PO_4, 1 mg/ml *o*-nitrophenyl-β-D-galactoside, 2.7 μl/ml β-mercaptoethanol) was added, and the reactions were incubated at 37 °C until solution developed a stable pale yellow color. The reactions were terminated by the addition of 500 μl of 1 M Na_2CO_3, and the incubation time was recorded. The samples were centrifuged to remove cell debris, the A_{400} was measured for the supernatant, and the Miller units were calculated as described (30).

RESULTS

Stable Inactive Promoter-proximal Transcription Elongation Complexes Are Formed on rplN and ompX Promoters during in Vitro Transcription in the Absence of Gre Factors—In experiment shown in Fig. 1*A*, the effect of GreA and GreB on *in vitro* transcription from an *rplN* promoter-containing linear DNA fragment was investigated. Transcription reactions were performed under conditions described in the previous work (23) but with two important modifications (see also "Experimental Procedures"). First, the length of transcription unit was much

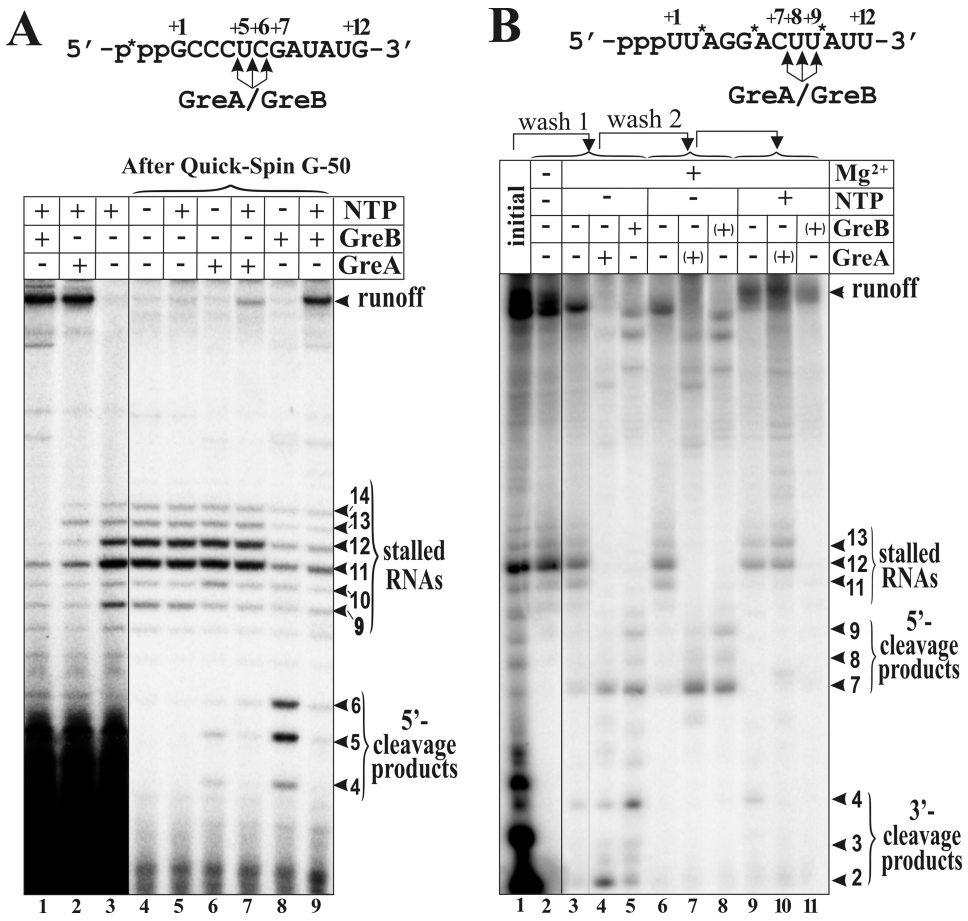

FIGURE 1. ***In vitro* transcription analysis of stalled promoter-proximal TCs generated on linear P*rplN* (*A*) and P*ompX* (*B*) DNA templates.** Each panel is an autoradiogram of the denaturing 23% PAGE of radiolabeled RNA products. Transcription reactions were conducted under conditions specified in details under "Experimental Procedures." Positions of the run-off, stalled, and cleaved RNA products are indicated on the *right*. Schematic diagrams indicating positions of GreA- and GreB-induced RNA cleavages in stalled TCs formed at P*rplN* and P*ompX* are shown above each autoradiogram. Here and elsewhere, an *asterisk* designates the position of radioactive phosphate. *A*, purification, transcript cleavage, and RNA extension assays of stalled radiolabeled TCs formed at P*rplN* [−84;+77] DNA by wt RNAP in solution. *Lanes 1–3*, multiround run-off transcription reactions carried out with 30 μM NTPs and [γ-P^{32}]GTP in the absence (*lane 3*) or presence of 4 μM GreA (*lane 2*) or 0.4 μM GreB (*lane 1*). Each lane represents $^1/_{10}$ of the initial material before Quick-Spin chromatography. *Lanes 4–9*, stalled promoter-proximal TCs purified by Quick-Spin G-50 gel filtration subjected to transcript cleavage (*lanes 4*, *6*, and *8*) and NTP-chase (*lanes 5*, *7*, and *9*) reactions in the absence (*lanes 4* and *5*) or presence of 4 μM GreA (*lane 6* and *7*) and 0.4 μM GreB (*lanes 8* and *9*). Each lane represents $^1/_6$ of the material loaded on Quick-Spin G-50. *B*, purification, transcript cleavage, and RNA extension assays of stalled radiolabeled TCs formed at P*ompX* [−188;+65] DNA using His-tagged RNAP immobilized on nickel-agarose beads. Each lane represents ~$^1/_{12}$ of the initial bead suspension, except for *lanes 3*, *4*, and *11*, which contain less material because of mechanical losses during washing procedures. *Lanes 1* and *2*, run-off transcription reaction carried out with 30 μM NTPs and [α-P^{32}]ATP in the absence of Gre factors before and right after first washing, respectively. *Lanes 3–8*, washed stalled promoter-proximal TCs were subjected to transcript cleavage reactions in the absence (*lane 3*) or presence of GreA (*lane 4*) or GreB (*lane 5*), followed by additional round of washing to remove cleaved 3′-terminal RNA fragments (*lanes 6–8*, respectively). *Lanes 9–11*, reactivated TCs carrying 5′-terminal cleavage products after second round of washing were chased in the presence of 100 μM NTPs. The presence of residual amounts of GreA and unwashed tightly bound GreB in TCs is indicated by (+) in *lanes 7*, *8*, *10*, and *11*.

shorter than before, which allowed simultaneous detection of abortive and full-length transcripts on the same gel. The second difference was that transcripts initiated from P*rplN* were 5′-terminally labeled with [γ-^{32}P]GTP, which allowed direct comparison of the relative amounts of short and long transcripts synthesized. As can be seen, almost no full-sized *rplN* transcript was formed by RNAP in the absence of cleavage factors (Fig. 1*A*, *lane 3*). Instead, a series of transcripts whose lengths ranged from 9 to 14 nt were formed, with 11-nt-long transcript being the most prominent. The absence of full-sized transcripts was not caused by a general inability of the RNAP holoenzyme (which was purified from *greA*$^-$ *greB*$^-$ cells) to transcribe productively, because the enzyme efficiently produced full-length run-off products on several control templates harboring promoters such as T7 A1, T5 N25, and *rrnB* P1 (data not shown). In the presence of either GreA or GreB, the abundance of short transcripts significantly decreased (*lanes 2* and *1*, respectively); concomitantly, the full-sized *rplN* transcript appeared.

To determine the nature of short *rplN* transcripts, reactions carried out in the absence of Gre factors were passed through a Sephadex G-50 column, which removes unincorporated NTPs and RNA not associated with RNAP from transcripts that are part of the transcription complex (TC). As can be seen (Fig. 1*A*, *lane 4*), most of NTPs were retained by column (as judged by the disappearance of [γ-^{32}P]GTP), whereas most of the 9–14-nt-long transcripts eluted in the void volume, indicating that they are stably associated with RNAP. Nevertheless, transcripts in purified TCs could not be chased by the addition of NTPs (*lane 5*), indicating that *rplN* TCs containing the 9–14-nt-long transcripts are transcriptionally inactive. The addition of GreB to inactive complexes led to a substantial decrease in the amount of 9–14-nt-long transcripts (*lane 8*) and accumulation of radioactive (and, therefore, 5′-terminal) 4–6-nt-long cleavage products. The effect of GreA was similar (*lane 6*) but much less pronounced. Radioactive cleaved RNAs remained associated with RNAP and could be extended into run-off transcripts by the addition of NTPs (*lanes 7* and *9*). Again, the stimulatory effect of GreA on full-sized transcript synthesis was much less than that of GreB (and appeared to correlate with the extent of accumulation of transcript cleavage products).

Similar analysis was carried out for transcripts generated from an *ompX* promoter-containing linear DNA fragment (Fig. 1*B*). Primer extension analysis of P*ompX* transcripts revealed that RNAP initiates transcription with UTP corresponding to the position labeled *+1* in Fig. 1*B*, both *in vivo* and *in vitro* (data not shown). The unavailability of [γ-^{32}P]UTP precluded us

from terminally labeling P*ompX* transcripts. Instead, as in the previous work, we used internal label [α^{32}-P]ATP, which is first found in the +3 position of the transcript. Both Gre factors strongly stimulated production of full-sized transcripts from the *ompX* promoter at conditions of a steady-state multiple-round transcription assay (Ref. 23 and data not shown). In the absence of Gre factors, several short transcripts were synthesized, among which 3-, 5-, and 12-nt-long transcripts were most prominent. However, unlike in the case of transcription from P*rplN,* the full-sized *ompX* transcript was also produced (Fig. 1*B*, *lane 1*). Because of the presence of adenines in multiple positions of the *ompX* transcription unit, specific radioactivity of the run-off product is much higher than that of the 12-nt-long RNA (*lane 1*). For this reason and because of our inability to cleanly separate the run-off product from *ompX* TCs by Sephadex G-50 gel filtration, we identified transcripts associated with RNAP by performing immobilized *in vitro* transcription reactions using hexahistidine-tagged RNAP and nickel-nitrilotriacetic acid-agarose (35). As can be seen (*lane 2*), washed immobilized transcription reactions lacked unincorporated [α-^{32}P]ATP and 3–10-nt-long RNAs that must correspond to true abortive transcripts. In contrast, 11–13-nt-long RNAs remained stably associated with RNAP; a substantial amount of full-sized transcripts also remained bound to RNAP, which we attribute to the formation of non-native complexes at the end of the DNA template (36). The addition of Gre factors to washed immobilized TCs led to the appearance of cleavage products ranging in length from 9 to 2 nt (*lanes 4* and 5). Unlike the situation observed with P*rplN*, both GreA and GreB were similarly active in *ompX* transcripts cleavage, although the pattern of cleavage products differed. Complexes containing the full-sized transcript and presumably stalled at the end of the template were also subject to factor-dependent cleavage, although this was not investigated further.

An additional round of washing of immobilized P*ompX* TCs after Gre-induced cleavage revealed that short cleavage products were removed, whereas longer, 7–9-nt-long products remained associated with TCs (*lanes 7* and *8*). Thus, in the case of P*ompX*, the cleavage occurs within 2–4 nucleotides from the 3′ end of RNA in stalled transcription complexes (recall that P*ompX* transcripts are labeled with [α-^{32}P]AMP in positions +3, +6, and +10, as indicated in the *scheme* shown at the *top* of Fig. 1*B*).

The addition of NTPs to washed TCs containing 11–13-nt-long transcripts did not lead to transcript elongation (*lane 9*). In contrast, TCs containing 7–9-nt-long RNA cleavage products could be chased (*lanes 10* and *11*). Chasing of washed TCs obtained after GreA cleavage led to very efficient formation of complexes stalled at positions +12/+13 (*lane 10*). No such complexes were formed when washed TCs formed upon GreB cleavage were chased (*lane 11*, only full-sized transcripts were observed). Although this was not further investigated, we attribute this difference to the lower affinity of GreA to RNAP, which leads to its complete removal during the washing step. In contrast, GreB, which binds RNAP much stronger (37, 38), is apparently able to at least partially withstand the washing procedure. Residual GreB then allows RNAP to read through the block at positions +12/+13 of the *ompX* transcription unit.

In summary, the results of our analysis indicate that on the two Gre-dependent promoters studied here, promoter-proximal inactive TCs are formed. These inactive/stalled TCs can be reactivated by the addition of Gre factors and may thus correspond to previously described dead end or arrested complexes (3, 12, 13, 39). When analysis similar to the one described above was performed with several templates driven by well studied *E. coli* RNAP promoters such as T7 A1, *rrnB* P1, and T5 N25, no stalled or arrested promoter-proximal TCs that were sensitive to Gre factors could be detected (data not shown). Thus, formation of promoter-proximal stalled TCs may be a common feature of those promoters whose activity is stimulated by Gre factors.

Inactive/Stalled Promoter-proximal TCs Formed on PrplN and PompX Are backtracked—Previously characterized arrested TCs were shown to form when the RNAP catalytic center disengages from the 3′ end of the nascent transcript and the enzyme backslides along the DNA (12, 13). The "extra" RNA proximal to the 3′ end is likely accommodated in the RNAP secondary channel, which also accepts the transcript cleavage factors (28, 40). To determine the position of the catalytic center in promoter-proximal inactive/stalled TCs formed at P*rplN*, we performed localized Fe^{2+}-mediated hydroxyl radical cleavage reactions (12) using gel-purified 5′-terminally radiolabeled stalled TCs containing Fe^{2+} instead of Mg^{2+} in RNAP catalytic center (Fig. 2). Under conditions when hydroxyl radicals were generated by the addition of dithiothreitol, radioactive RNAs of 4, 5, and 6 nt in length started to accumulate (Fig. 2, *lane 4*). These RNAs were not the products of intrinsic nucleolytic activity of RNAP because no cleavage was observed in the presence of Mg^{2+} (*lane 3*). Also, the appearance of these products was decreased when reactions were supplied with Fe^{2+} chelator EDTA (*lane 5*), indicating that the observed cleavage products were specifically caused by Fe^{2+} ions. The efficiency of Fe^{2+}-mediated reactions was relatively low (1–2% of the initial inactive/stalled TCs), which is likely to be due to degradation of the RNAP β and β' subunits and subsequent inactivation of RNAP by hydroxyl radicals (41). The sizes of cleaved 5′-radiolabeled RNAs match the sizes of cleavage products observed when stalled P*rplN* TCs are treated with Gre factors (Fig. 1*A*). Based on these results, we conclude that stalled promoter-proximal TCs on P*rplN* are backtracked by ~5–7 bp.

To reveal the size and position of the transcription bubble in promoter-proximal stalled TCs, they were probed with $KMnO_4$ followed by primer extension analysis (Fig. 3). In complexes formed by RNAP on P*rplN* in the absence of NTPs, little or no $KMnO_4$-sensitive bands were detected (Fig. 3*A*, *lane 3*; see also supplemental Fig. S1). This was due to instability of P*rplN* open promoter complexes (data not shown), a situation previously observed for ribosomal RNA promoters (30). The addition of GTP, CTP, and UTP to the reaction allows transcription to proceed to G^{+7} (position +8 in the P*rplN* initial transcribed sequence specifies an A; Fig. 1*A*), which leads to formation of an active promoter-proximal complex carrying a 7-nt-long RNA (TC-7G; supplemental Fig. S1). $KMnO_4$ probing of TC-7G revealed that in the nontemplate DNA strand there were two

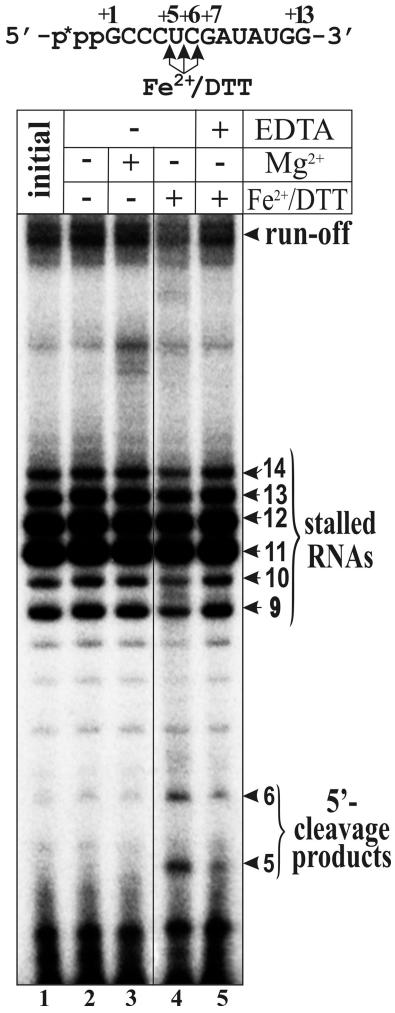

FIGURE 2. **Localized Fe^{2+}-mediated hydroxyl radical mapping of the position of the catalytic center in promoter-proximal arrested TCs at P*rplN*.** Shown is an autoradiogram of the denaturing 23% PAGE separating short radiolabeled RNA cleavage products. Purified arrested TCs carrying [γ-P^{32}]GTP-radiolabeled 9–14-nt-long transcripts (*lane* 1) were incubated in the absence of metal ions (*lane 2*) or in the presence of 10 mM Mg^{2+} (*lane 3*), 0.1 mM Fe^{2+} together with 1 mM dithiothreitol (*lane 4*), or 50 mM EDTA (*lane 5*). The positions of stalled/arrested RNAs and 5′-terminal cleavage products are indicated on the *right*. A schematic diagram indicating positions of Fe^{2+}-induced hydroxyl-radical cleavages in stalled/arrested 13-meric RNA is shown *above* the autoradiogram.

sensitive thymidines at positions +5, and +9 and one weakly sensitive thymidine at position −6 relative to the transcription start point (Fig. 3*A*, *lane 4*). Additional bands seen on the gel and corresponding to cytidines at positions +3/+4 and thymidine at +11 were not the result of $KMnO_4$ modification but were due to stalling of DNA polymerase at and around the modified thymidines during primer extension reaction (see "Experimental Procedures"). Consistent with this interpretation, bands corresponding to these cytidines were not observed during direct visualization of $KMnO_4$-induced modification by piperidine treatment of end-labeled DNA template (supplemental Fig. S1). The pattern of $KMnO_4$ modification in TC-7G did not change in the presence of GreA (*lane 5*). Probing of reactions supplied with all four NTPs, a condition when inactive promoter-proximal complexes form (Figs. 1*A* and 2), revealed a similar pattern of modification, although the reactivity of thymidine at downstream position +9 appeared to be decreased (Fig. 3*A*, *lane 7*). Importantly, the addition of GreA led to almost total disappearance of $KMnO_4$-sensitive bands (*lane 7*). The addition of GreA-D41E, a mutant that binds transcription complexes normally but is unable to induce transcript cleavage (23, 28) had no such effect (*lane 8*).

$KMnO_4$ probing of complexes on P*ompX* was also performed (Fig. 3*B* and supplemental Fig. S2). Unlike P*rplN*, $KMnO_4$ sensitivity of thymidines within open promoter complexes (*i.e.* in the absence of NTPs) is readily observed on this promoter (Fig. 3*B*, *lane 6*). As revealed by primer extension analysis, thymidines at template strand positions −11 and −9 and partially at positions −5/−2 are sensitive to the reagent. In the presence of NTPs, a condition when stalled promoter-proximal complexes form (Fig. 1*B*), the sensitivity of thymidines at positions −11 and −9 to $KMnO_4$ was abolished. Instead, thymidines at positions −2/−5 become highly reactive (Fig. 3*B*, *lane 5*). The addition of GreA (*lane 4*) but not the inactive D41E mutant (*lane 3*) led to disappearance of $KMnO_4$ sensitivity at positions −5/−2. Neither factor appreciably altered the residual sensitivity of thymidines at positions −11 and −9, which must be due to formation of unproductive open complexes that fail to leave the promoter in the presence of NTPs.

The summary of $KMnO_4$ probing on both the template and nontemplate strands for each of the two promoters studied here is shown in the *right panels* of Fig. 3 (*A* and *B*, respectively) (see also supplemental Figs. S1 and S2). On P*rplN*, upon transition of transcriptionally active complex TC-7G into stalled inactive TCs, the transcription bubble shrinks in size from ~18–19 to ~15 bp; the front edge of the bubble moves backward from +8/+9 to +5, whereas the rear edge of the bubble remains at −10/−11 (Fig. 3*A*, *right panel*). On the other hand, during transition from an open promoter complex to stalled inactive TCs on P*ompX*, the transcription bubble decreases in size from ~14 to ~12 bp, whereas both the rear and the front edge of the bubble move forward from −10/−11 to −2 and from +1/+3 to +9/+10, respectively (Fig. 3*B*, *right panel*). Together, the data presented are consistent with the idea that on both promoters, stalled promoter-proximal TCs are backtracked. This conclusion is further supported by the results of ExoIII nuclease footprinting experiments designed to reveal the positions of the front and rear edges of RNAP on DNA in TCs stalled at P*ompX* and P*rplN* (data not shown). Because promoter-proximal stalled TCs are 1) unable to elongate nascent transcripts even upon prolonged incubations with high concentrations of NTPs, 2) rescued by transcript cleavage factors, and 3) backtracked, they indeed correspond to previously described arrested elongation complexes (3, 12, 13, 39).

The Strength of the σ^{70} Subunit Interaction with the RNAP Core Affects the Formation of Promoter-proximal Arrested TCs—Previously described promoter-proximal RNAP pausing (29, 32, 43–46) is caused by σ "hopping," a process when the σ subunit region 2, as a part of the RNAP holoenzyme, recognizes a region in the initial transcribed sequence of the promoter that is similar to the −10 promoter element consensus sequence (29). During hopping, the contacts of σ with the *bona fide* −10 promoter element are broken, and new contacts are established

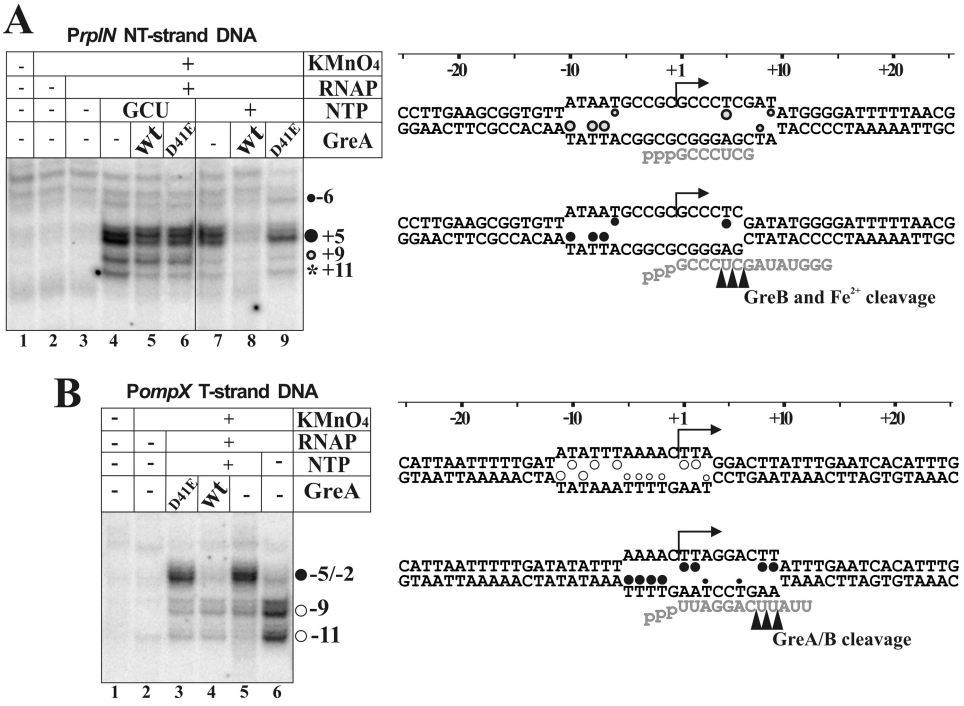

FIGURE 3. **$KMnO_4$ footprinting of the transcription bubble in stalled/inactive promoter-proximal TCs generated on plasmid DNA templates pES-rpIN (*A*) and pES-ompX (*B*).** The *left panels* are autoradiograms of 6% sequencing PAGE of the products of primer extension reactions after treatment with $KMnO_4$. *A*, thymidine modifications in the nontemplate DNA strand of transcription complexes obtained on P*rplN* in the absence or presence of limited (GTP, CTP, and UTP) and full set of NTPs with and without wt GreA or mutant GreA-D41E. *B*, thymidine modifications in the template DNA strand of transcription complexes obtained on P*ompX* in the absence or presence of NTPs with and without wt GreA or mutant GreA-D41E. The *right panels* are schematic diagrams showing the positions of strong (*large circles*) and weak (*small circles*) reactivity of thymidines to $KMnO_4$ in both DNA strands of open promoter complex, in transcriptionally active promoter-proximal TC-7G, and in stalled/inactive promoter-proximal TC (*open*, *shaded*, and *filled circles*, respectively). Transcription start site (+1) is indicated on each diagram by a *thin bent arrow*, and the sites of GreA/B- and Fe^{2+}-induced RNA cleavages in stalled promoter-proximal TCs are shown by *black arrowheads*.

with the downstream "−10-like" element, which is present in a single-stranded form because it is part of the transcription bubble. The interaction of σ with the "sticky" downstream −10 like element leads to pausing. Inspection of the P*rplN* and P*ompX* initial transcribed sequences did not reveal any similarities with the −10 promoter element consensus sequence. Likewise, analysis of the initial transcribed sequences of other GreA-responsive promoters (23) revealed no similarities to the −10 consensus sequence (we also failed to detect any common sequences for these promoters other than promoter consensus elements, data not shown). To elucidate the role of the σ subunit in the formation of promoter-proximal arrested TCs on Gre-stimulated promoters, we performed *in vitro* transcription experiments using RNAP holoenzyme reconstituted with σ^{70} harboring a L402F substitution. Previous work demonstrated that this substitution decreases the strength of σ^{70} interaction with the core enzyme (29). As can be seen from Fig. 4*A*, during multiround transcription on the P*ompX* template in the absence of Gre factors, RNAP holoenzyme harboring σL402F produced considerably fewer transcripts corresponding to promoter-proximal arrested TCs (and more run-off products) than the wt holoenzyme (compare *lanes 1* and *3*). On P*rplN*, the amount of RNAs corresponding to promoter-proximal arrested TCs was similar for both holoenzymes; however, ~3.5 times more of the full-sized transcripts were produced by the mutant RNAP (compare *lanes 5* and *7*). The effect was specific, because both holoenzymes transcribed equally well from the T7 A1 promoter (data not shown). The addition of GreA decreased the amount of arrested TCs formed and increased the production of full-sized transcripts by wt RNAP on both templates, as expected (compare *lanes 1* and *2* with *lanes 5* and *6*). The addition of GreA prevented transcriptional arrest of σL402F-RNAP on P*rplN* and increased the amount of run-off (compare *lanes 7* and *8*), although not as much as in the case of the wt RNAP (compare *lanes 5* and *6*). Because on P*ompX* only a small fraction of σL402F-RNAP undergoes arrest (*lane 3*), the stimulatory effect of GreA on full-sized transcript production was only 1.4-fold (*lane 4*).

The significant amount of short (10–13-nt-long) transcripts formed by the σL402F-RNAP on the P*rplN* template (Fig. 4*A*, *lane 7*) could, in principle, be due to decreased stability of promoter-proximal arrested TCs formed by the mutant holoenzyme. Such decreased stability would lead to increased production of full-length transcripts by allowing faster RNAP recycling. If promoter-proximal arrested TCs formed by the mutant RNAP were less stable, then in a single-round transcription assay, open promoter complexes formed by the mutant enzyme would have produced fewer full-sized transcripts than the same amount of open complexes formed by the wt RNAP. Further, in this scenario, RNA in stalled complexes formed by the wt RNAP should remain bound to the enzyme, whereas corresponding RNAs formed by the mutant enzyme should dissociate from the complex. In Fig. 4 (*B* and *C*), the results of a single-round transcription experiment on P*rplN* are presented. A mixture of NTPs and rifampicin, a drug that prevents RNAP escape into elongation, was added to preformed P*rplN* open complexes formed by the wt or the mutant holoenzyme. RNAP molecules that manage to elongate RNA past trinucleotide become resistant to rifampicin and can complete a single round of transcription; however, further rounds of productive transcription are prevented. As can be seen, the mutant RNAP produced *fewer* transcripts corresponding to promoter-proximal arrested TCs and *more* full-sized transcripts than the wt RNAP (compare *lanes 1* and *4*). Quantitative analysis showed that although only ~12% of the wt RNAP molecules reach the end of the template with 88% becoming arrested, more than 50% of transcripts initiated by the mutant RNAP holoenzyme became full-sized (Fig. 4*C*).

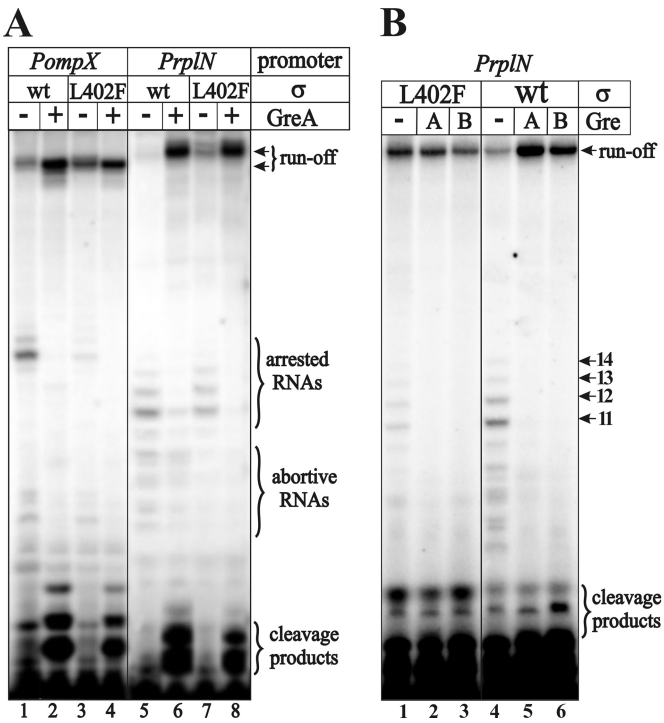

FIGURE 4. ***In vitro* transcription analysis of promoter-proximal arrested TCs generated on linear P*rplN* and P*ompX* DNA templates by wt RNAP holoenzyme and mutant σL402F-RNAP.** *A* and *B* are autoradiograms of the denaturing 23% PAGE. *A*, multiround transcription assay in the presence and absence of 4 μM GreA. *B*, single-round transcription reactions at P*rplN* in the presence of rifampicin, with and without wt GreA and GreB. Positions of run-off, abortive, and arrested RNAs as well as products of GreA-induced cleavage are indicated on the *right*. *C*, quantitative analysis of the amounts of run-off (*black bars*) and arrested RNAs (*gray bars*) (expressed as relative units, *RU*) formed during single-round transcription reactions by wt RNAP (*top panel*) and mutant RNAP (*bottom panel*) in the absence and presence of GreA and GreB.

These results suggest that by weakening σ^{70}-core interactions, the σL402F mutant improves the readthrough efficiency (*i.e.* transcripts initiated by the mutant RNAP fall into the arrested state at promoter-proximal sites less often), thereby accelerating promoter escape and increasing productive transcription from Gre-dependent promoters studied here. Indeed, in the presence of NTPs, $KMnO_4$ modification of thymidines at nontemplate strand positions +5/+9 of P*rplN* and +8/+9 of P*ompX* indicative of arrested TCs was much less efficient in reactions containing the mutant holoenzyme than in the wt RNAP-containing reactions. Nevertheless, in both cases, the $KMnO_4$-reactive thymidines were sensitive to GreA and GreB (supplemental Fig. S3). Thus, we conclude that formation of promoter-proximal arrested TCs is determined, at least in part, by the strength of σ^{70} interaction with the core enzyme and may therefore involve σ hopping despite the apparent absence of sequences that could be recognized by σ in arrested TCs.

Promoter-proximal Arrested TCs Are Formed on PrplN and PompX in Vivo—Using plasmid-borne *PrplN*- and P*ompX-lacZ* fusion reporter constructs, we determined that wt GreA but not the cleavage-defective GreA-D41E mutant stimulates the production of β-galactosidase ~7- and ~2-fold, respectively (Fig. 5*A*). To determine whether GreA-dependent stimulation of P*rplN* and P*ompX* involves formation of promoter-proximal arrested complexes *in vivo*, $KMnO_4$ probing of *greA*$^-$*greB*$^-$ or isogenic *greA*$^+$*greB*$^-$ cells harboring P*rplN*- and P*ompX*-reporter plasmids was carried out (Fig. 5*B*). As can be seen, on both promoters robust $KMnO_4$-sensitive thymidines were only observed in the absence of Gre factors. In the case of P*rplN*, $KMnO_4$-sensitive thymidine at position +5 of the nontemplate strand (Fig. 5*B*, *left panel*, *lane 3*) corresponded to the one observed *in vitro* for promoter-proximal arrested TCs (compare with Fig. 3*A*). In the case of P*ompX*, $KMnO_4$-sensitive thymidines at positions −2/−5, −9, and −11 of the template strand (Fig. 5*B*, *right panel*, *lane 3*) corresponded to promoter-proximal arrested TCs and open complex, respectively (compare with Fig. 3*B*). $KMnO_4$-sensitive thymidines at −9 and −11 corresponding to open complexes became more prominent when cells were treated with rifampicin prior to $KMnO_4$ treatment (compare *lanes 3* and *5*), an expected result because rifampicin does not affect open promoter complex formation but prevents promoter escape. In the presence of GreA, the efficiency of $KMnO_4$ modification of thymidines corresponding to promoter-proximal arrested TCs on both promoters decreased (Fig. 5*B*, *right panel*, *lane 4*, and *left panel*, *lanes 4* and *6*), whereas efficiency of modification of thymidines corresponding to open complex on P*ompX* was unaffected (compare *lanes 5* and *6*). We therefore, conclude that 1) promoter-proximal arrested TCs form on P*rplN* and P*ompX in vivo* and 2) GreA, through its transcript cleavage activity, reduces the formation of these complexes and thereby stimulates gene expression. By extension, we propose that Gre-dependent stimulation of transcription not only from P*rplN* and P*ompX* but from at least some other Gre-dependent promoters revealed in our previous work (23) is due to suppression of formation and reactivation of promoter-proximal arrested TCs.

Signal for Promoter-proximal Arrest at PrplN Is Bipartite and Requires Two Elements: the Extended −10 Box and the Initial Transcribed Region from +2 to +6—To investigate the role of different promoter elements in formation of arrested TCs at P*rplN*, we constructed a set of 15 promoter variants where the upstream (promoter region) and the downstream (initial transcribed region, ITR) segments of P*rplN* are replaced either with the corresponding parts of the T7 A1 promoter or with segments of random DNA sequence (Fig. 6). The transcriptional activities of resulting promoter variants were analyzed by single- and multiround run-off transcription assays in the absence or in the presence of Gre factors. The ability of different promoter variants to induce formation of promoter-proximal arrested TCs (and susceptibility of arrested TCs to GreA) was examined by comparing the patterns of short RNA products (5–20 nt long) in transcription reactions before and after puri-

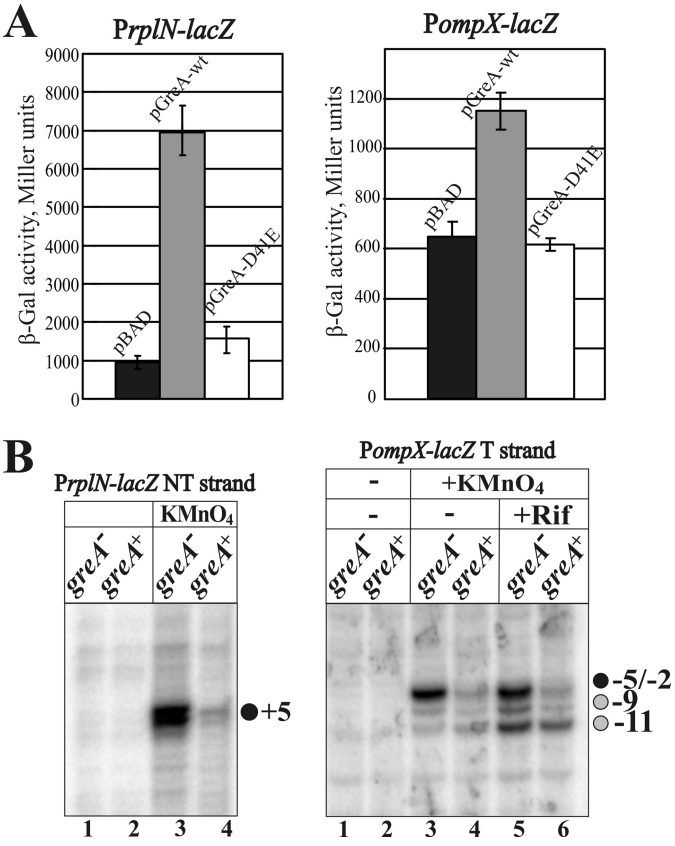

FIGURE 5. ***In vivo* analysis of promoter-proximal arrest at P*rplN* and P*ompX*.** *A*, β-galactosidase activity assay (expressed in standard Miller units) for plasmid-borne P*rplN-lacZ* (*left panel*) and P*ompX-lacZ* (*right panel*) fusion reporter constructs in *E. coli* strains expressing wt GreA or inactive GreA-D41E mutant, or carrying control vector pBAD. *B*, detection of promoter-proximal transcriptional arrest *in vivo* by $KMnO_4$ treatment of *greA*$^-$/*greB*$^-$ strain BW32645 or isogenic *greA*$^+$*greB*$^-$ strain BW32613 carrying reporter plasmid pES-rplN (*left panel*) or pES-ompX (*right panel*). $KMnO_4$-sensitive thymidine at position +5 of the nontemplate strand in pES-rplN and thymidines at positions −2/−5, −9, and −11 of the template strand in pES-ompX are visualized by primer extension analysis (see "Experimental Procedures"). Rifampicin was added 5 min before $KMnO_4$ treatment in *lanes 5* and *6*.

fication through Quick-Spin gel filtration columns (see "Experimental Procedures").

First, we found that swapping the upstream (from −84 to +1, construct 14) or the downstream (from +2 to +45, construct 9) parts of P*rplN* with the corresponding parts of T7 A1 had only a small (1.7–2.5-fold) stimulatory effect on overall transcriptional activity but effectively eliminated transcriptional arrest at both hybrid promoters (Fig. 6, compare constructs 1, 9, 14, and 15). Thus, the signal for promoter-proximal transcriptional arrest is (at least) bipartite and is located both in the upstream and the downstream portions of P*rplN*. More detailed analysis of the upstream part of P*rplN* revealed that deletion of A/T-rich "UP-like" sequence (located around position −45, construct 3), alone or together with the −35 element (construct 4), or introduction of the consensus −35 element sequence into P*rpllN* (construct 2) had only a moderate effect on promoter activity or efficiency of transcriptional arrest (constructs 2–4). Similar results were observed when we introduced multiple substitutions in the discriminator region (positions −5 to −1) or replaced a G at the transcription start site (+1) to an A (constructs 6 and 7, correspondingly). However, substitution of a TG dinucleotide upstream of the −10 element (positions −13/−14) with a CC dinucleotide caused >20-fold decrease in promoter activity and the disappearance of arrested TCs (construct 5). The result indicates that P*rplN* belongs to the "extended −10" promoter class and that the extended TG-element constitutes a part of the signal for promoter-proximal arrest. Other upstream promoter elements of P*rplN* do not play a significant role in either promoter activity or early transcriptional arrest. Further dissection of the downstream (ITR) part of P*rplN* using substitutions in 5-bp-long segments encompassing a region from +2 to +21 revealed that changes in four positions (+2, +4, +5, and +6) in the wt ITR sequence led to nearly complete disappearance of arrested TCs (construct 10), whereas sequence alterations between positions +7 to +11 (construct 11), +12 to +16, and +17 to +21 (constructs 12 and 13) had only moderate or negligible effects. Thus, the second part of the signal determining promoter-proximal transcriptional arrest at P*rplN* is located between positions +2 and +6 of the ITR.

In the presence of GreA, the formation of abortive RNA and arrested TCs (wherever arrest took place) in all of the studied promoter constructs was significantly reduced with concomitant increase in the amount of run-off product, both in single- and multiround transcription assays (Fig. 7*A* and data not shown). For most studied templates where arrested TCs were formed, the stimulatory effect of GreA was in the range of 6–13-fold (Fig. 7*B*). Noticeably, even on templates where arrest did not occur, GreA increased the amount of run-off 3–7-fold. The only exception was the wt T7 A1, where the effect was only 2-fold (Fig. 7*B*). These observations are consistent with results of Hsu *et al.* (9), who found that various deviations from the natural "optimized" sequence of ITR interfere with efficiency of promoter escape through multiple mechanisms, such as increased abortive cycling, formation of "moribund" initiation complexes, etc.

DISCUSSION

The principal observation of this work is that during transcription initiation in the absence of transcript cleavage factors Gre, at promoters *rplN* and *ompX*, *E. coli* RNAP falls into a promoter-proximal arrested state that impedes production of full-length transcripts both *in vitro* and *in vivo*. Promoter-proximal transcriptional arrest occurs when RNAP synthesizes 9–14-nt-long transcripts and backtracks by 5–7 (P*rplN*) or 2–4 (P*ompX*) nucleotides. GreA and GreB prevent arrest at P*rplN* and P*ompX* by inducing RNA cleavage at the onset of arrested TC formation and stimulate productive transcription by allowing RNAP to use the 5′ end proximal transcript cleavage products as primers for productive transcription. Both factors can cleave and reactivate arrested TCs at P*ompX*, but only GreB can reactivate arrested TCs at P*rplN*. The difference between the action of Gre factors is apparently due to the fact that GreA can cleave RNA only by small 2–4-nt-long fragments, whereas GreB is able to cleave both in small and in large, 4–18-nt-long increments (1–3, 13).

The two arrested TCs described here are clearly different from promoter-proximal paused TCs that have been previously observed at several bacterial and bacteriophage pro-

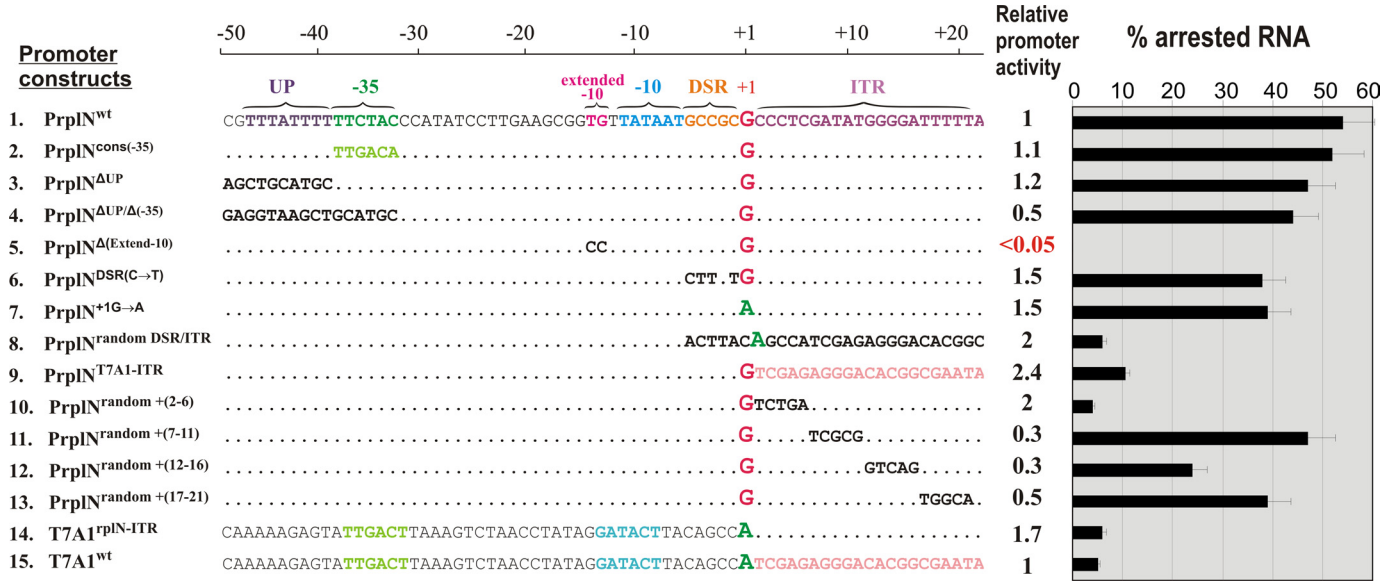

FIGURE 6. **Relative *in vitro* transcriptional activity and efficiency of arrested complex formation for wt and mutant P*rplN* and P*rplN/T7A1* promoter variants.** Nucleotide positions identical to that of wt P*rplN* are shown as *dots*. Promoter elements of P*rplN* that are mutagenized or swapped between P*rplN* and P*T7A1* are indicated on sequence alignment by *different colors*. Relative promoter activity was measured in a multiround transcription assay under standard conditions (10 μl of TB containing 0.1 pmol of DNA fragment, 0.3 pmol of *E. coli* RNAP holoenzyme, 100 μM NTPs, 0.165 μM [α-P^{32}]ATP (3000 Ci/mmol)) after 15 min of incubation at 37 °C in the presence of 4 μM GreA and is expressed in relative units. 1 unit is defined as the amount of run-off product synthesized on wt P*rplN* DNA. For each promoter, the amount of run-off and total RNA was measured in a single-round transcription reaction (see "Experimental Procedures") carried out in the presence of 30 μM NTPs and 0.2 μM [γ-P^{32}]GTP or [γ-P^{32}]ATP (4500 Ci/mmol). The percentage of arrested RNA of the total RNA was calculated based on the amounts of 9–14-nt-long transcripts remaining in complex with RNAP after the Quick-Spin chromatography.

moters (29, 32, 43–46). The principal difference between promoter-proximal arrested and paused TCs is that the latter exist only transiently and eventually clear the pause site. In contrast, arrested TCs formed on P*rplN* and P*ompX* are permanently inactive in the absence of Gre factors. In this, they are similar to two previously characterized arrested TCs that were obtained *in vitro*: one forming during unusual primer shift initiation at the ribosomal *rrnB*P1 promoter (3, 47) and another forming at phage T7 A1 promoter after prolonged incubation of an elongation complex containing 27-nt-long RNA in the absence of a substrate specified by the template position 28 (12, 13, 39). Unlike these artificially arrested TCs, promoter-proximal arrest at P*rplN* and P*ompX* takes place both *in vitro* and *in vivo* during "natural" initiation in the presence of all NTPs at high concentrations.

Promoter-proximal transcriptional arrest may occur through different mechanisms, which need not be mutually exclusive. First, the arrest may be caused by excessive DNA scrunching during promoter escape. The relief from scrunching, in the form of RNAP backtracking, may reposition short transcripts into an RNAP site that allows tight interaction with the enzyme and therefore prevents transcript dissociation. Second, the RNAP σ subunit can contribute to promoter-proximal arrest either by directly interacting with short transcripts in the backtracked conformation of the complex or through the hopping mechanism, although the latter must take place in the absence of appropriately located sequences with similarities to the −10 promoter element consensus in the initial transcribed regions of promoters studied here.

Be that as it may, we propose that formation of promoter-proximal inactive/stalled TCs is a common feature of promoters whose efficient transcription requires transcript cleavage factors. The molecular mechanisms of promoter-proximal stalling are as yet unknown. The signal for transcriptional arrest may be a complex function of the strength of RNAP-DNA/RNA interactions with different promoter elements and the structure of DNA (such as methylation, supercoiling, etc.). The contribution of these factors may be different at different promoters. Clearly, promoter-proximal arrest is a previously unrecognized yet likely common feature of many bacterial promoters and is a physiological target of regulation by transcript cleavage factors.

In fact, our results suggest that suppression of promoter-proximal arrest could be one of the main *in vivo* functions of GreA and GreB. The two other known anti-arrest mechanisms in the cell, including cooperative action of multiple RNAP molecules co-directionally transcribing through an arresting DNA site (48) and ATP-dependent dissociation of arrested TCs by transcription-coupled repair factor Mfd (42), may not work during promoter-proximal arrest. First, in the case of P*rplN* and P*ompX*, a significant portion of promoter DNA is still occupied by arrested RNAP (Fig. 3), preventing new transcription initiation and therefore rescue of arrested TC by the second RNAP molecule. In support of this, we found that arrested TCs are resistant to reactivation by excess of RNAP holoenzyme (data not shown). Second, the presence of σ-factor in promoter-proximal arrested TCs excludes Mfd from binding to and acting on arrested RNAP (42). Therefore, transcript cleavage reaction activated by GreA and GreB appears to be the only mechanism available in the cell to prevent and counteract promoter-proximal transcrip-

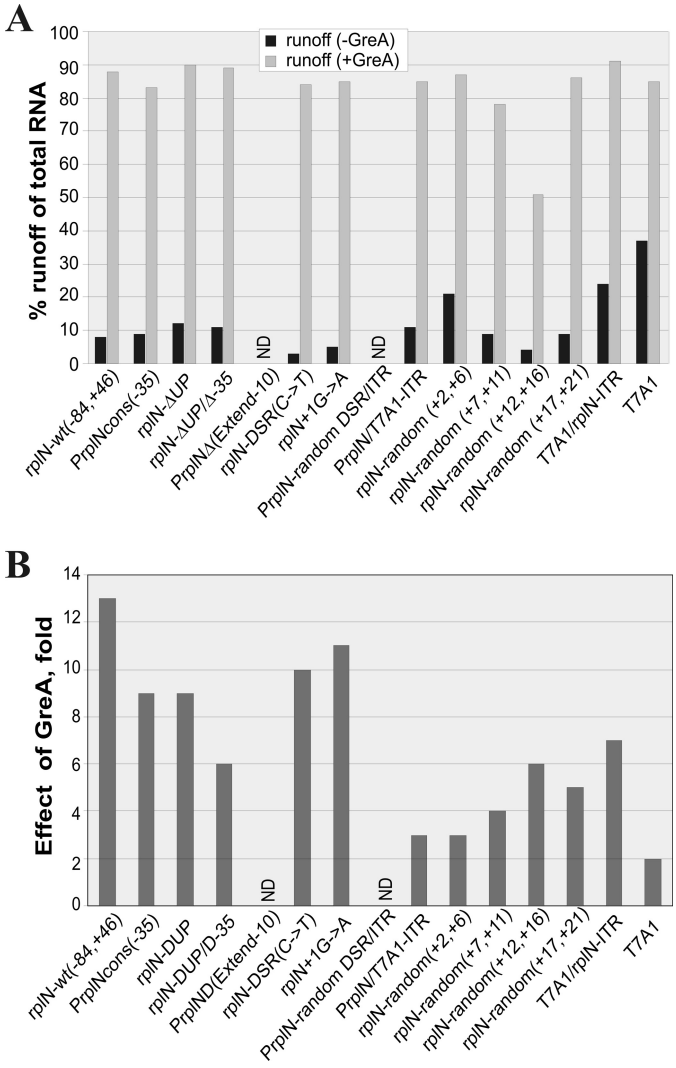

FIGURE 7. **Efficiency of the full-length run-off synthesis for wt and mutant P*rplN* promoter variants.** *A*, bar graphs show the percentage of run-off transcript of the total RNA synthesized in a single-round transcription assay (see legend for Fig. 6) in the absence (*gray bars*) or presence (*black bars*) of 4 μM GreA. *B*, bar graph shows the effect of GreA on the amount of run-off synthesis at different promoter variants. *ND*, data not determined because of a low amount of run-off product observed for P*rplNΔ(Extend-10*) and P*rplNrandomDSR/ITR* in a single-round transcription assay.

tional arrest, which may explain the high degree of conservation of transcript cleavage factors in evolution.

Very recently, an avalanche of data indicating the previously unrecognized commonality of transcription regulation via "transcription-poised" RNAP arrested early at the transcription unit in eukaryotes became available (reviewed in Ref. 34). Such a mechanism allows very rapid responses to environmental changes by "restarting" stalled transcription complexes and avoiding the need to assemble transcription initiation complexes *de novo*. Bacterial transcription units on which promoter-proximal arrested complexes responsive to Gre factors form are formally analogous to eukaryotic examples of regulation by transcription poising. Environmental conditions that lead to changes in gene expression by affecting the efficiency of promoter-proximal arrest are currently being investigated in our laboratories.

Acknowledgments—We are grateful to A. Parshin for providing purified wt and mutant Gre factors, M. Ozerova for preparation of GreA/GreB-free wt RNAP, J. W. Roberts for plasmid expressing σ-L402F, and R. Gourse for plasmid pRLG862. We also thank J. Lee for helpful discussions.

REFERENCES

1. Fish, R. N., and Kane, C. M. (2002) *Biochim. Biophys. Acta* **1577,** 287–307
2. Borukhov, S., Lee, J., and Laptenko, O. (2005) *Mol. Microbiol.* **55,** 1315–1324
3. Borukhov, S., Sagitov, V., and Goldfarb, A. (1993) *Cell* **72,** 459–466
4. Hawley, D. K., Wiest, D. K., Holtz, M. S., and Wang, D. (1993) *Cell Mol. Biol. Res.* **39,** 339–348
5. Erie, D. A., Hajiseyedjavadi, O., Young, M. C., and von Hippel, P. H. (1993) *Science* **262,** 867–873
6. Thomas, M. J., Platas, A. A., and Hawley, D. K. (1998) *Cell* **93,** 627–637
7. Hsu, L. M., Vo, N. V., and Chamberlin, M. J. (1995) *Proc. Natl. Acad. Sci. U.S.A.* **92,** 11588–11592
8. Susa, M., Kubori, T., and Shimamoto, N. (2006) *Mol. Microbiol.* **59,** 1807–1817
9. Hsu, L. M., Cobb, I. M., Ozmore, J. R., Khoo, M., Nahm, G., Xia, L., Bao, Y., and Ahn, C. (2006) *Biochemistry* **45,** 8841–8854
10. Fousteri, M., and Mullenders, L. H. (2008) *Cell Res.* **18,** 73–84
11. Toulmé, F., Mosrin-Huaman, C., Sparkowski, J., Das, A., Leng, M., and Rahmouni, A. R. (2000) *EMBO J.* **19,** 6853–6859
12. Nudler, E., Mustaev, A., Lukhtanov, E., and Goldfarb, A. (1997) *Cell* **89,** 33–41
13. Komissarova, N., and Kashlev, M. (1997) *Proc. Natl. Acad. Sci. U.S.A.* **94,** 1755–1760
14. Reeder, T. C., and Hawley D. K. (1996) *Cell* **87,** 767–777
15. Orlova, M., Newlands, J., Das, A., Goldfarb, A., and Borukhov, S. (1995) *Proc. Natl. Acad. Sci. U.S.A.* **92,** 4596–4600
16. Rudd, M. D., Izban, M. G., and Luse, D. S. (1994) *Proc. Natl. Acad. Sci. U.S.A.* **91,** 8057–8061
17. Weilbaecher, R. G., Awrey, D. E., Edwards, A. M., and Kane, C. M. (2003) *J. Biol. Chem.* **278,** 24189–24199
18. Nudler, E. (1999) *J. Mol. Biol.* **288,** 1–12
19. Zenkin, N., Yuzenkova, Y., and Severinov, K. (2006) *Science* **313,** 518–520
20. Trautinger, B. W., Jaktaji, R. P., Rusakova, E., and Lloyd, R. G. (2005) *Mol. Cell* **19,** 247–258
21. Mirkin, E. V., Castro Roa, D., Nudler, E., and Mirkin, S. M. (2006) *Proc. Natl. Acad. Sci. U.S.A.* **103,** 7276–7281
22. Feng, G. H., Lee, D. N., Wang, D., Chan, C. L., and Landick, R. (1994) *J. Biol. Chem.* **269,** 22282–22294
23. Stepanova, E., Lee, J., Ozerova, M., Semenova, E., Datsenko, K., Wanner, B. L., Severinov, K., and Borukhov, S. (2007) *J. Bacteriol.* **189,** 8772–8785
24. Goldman, S. R., Ebright, R. H., and Nickels, B. E. (2009) *Science* **324,** 927–928
25. Kapanidis, A. N., Margeat, E., Ho, S. O., Kortkhonjia, E., Weiss, S., and Ebright, R. H. (2006) *Science* **314,** 1144–1147
26. Revyakin, A., Liu, C., Ebright, R. H., and Strick, T. R. (2006) *Science* **314,** 1139–1143
27. Hsu, L. M. (2002) *Biochim. Biophys. Acta* **1577,** 191–207
28. Laptenko, O., Lee, J., Lomakin, I., and Borukhov, S. (2003) *EMBO J.* **22,** 6322–6334
29. Ko, D. C., Marr, M. T., Guo, J., and Roberts, J. W. (1998) *Genes Dev.* **12,** 3276–3285
30. Barker, M. M., Gaal, T., Josaitis, C. A., and Gourse, R. L. (2001) *J. Mol. Biol.* **305,** 673–688
31. Hernandez, V. J., and Bremer, H. (1990) *J. Biol. Chem.* **265,** 11605–11614
32. Hatoum, A., and Roberts, J. (2008) *Mol. Microbiol.* **68,** 17–28
33. Craig, M. L., Tsodikov, O. V., McQuade, K. L., Schlax, P. E., Jr., Capp, M. W., Saecker, R. M., and Record, M. T., Jr. (1998) *J. Mol. Biol.* **283,** 741–756
34. Nechaev, S., and Adelman, K. (2008) *Cell Cycle* **7,** 1539–1544

35. Kashlev, M., Nudler, E., Severinov, K., Borukhov, S., Komissarova, N., and Goldfarb, A. (1996) *Methods Enzymol.* **274,** 326–334
36. Nudler, E., Avetissova, E., Markovtsov, V., and Goldfarb, A. (1996) *Science* **273,** 211–217
37. Koulich, D., Orlova, M., Malhotra, A., Sali, A., Darst, S. A., and Borukhov, S. (1997) *J. Biol. Chem.* **272,** 7201–7210
38. Loizos, N., and Darst, S. A. (1999) *J. Biol. Chem.* **274,** 23378–23386
39. Surratt, C. K., Milan, S. C., and Chamberlin, M. J. (1991) *Proc. Natl. Acad. Sci. U.S.A.* **88,** 7983–7987
40. Zhang, G., Campbell, E. A., Minakhin, L., Richter, C., Severinov, K., and Darst, S. A. (1999) *Cell* **98,** 811–824
41. Mustaev, A., Kozlov, M., Markovtsov, V., Zaychikov, E., Denissova, L., and Goldfarb, A. (1997) *Proc. Natl. Acad. Sci. U.S.A.* **94,** 6641–6645
42. Park, J. S., Marr, M. T., and Roberts, J. W. (2002) *Cell* **109,** 757–767
43. Ring, B. Z., Yarnell, W. S., and Roberts, J. W. (1996) *Cell* **86,** 485–493
44. Brodolin, K., Zenkin, N., Mustaev, A., Mamaeva, D., and Heumann, H. (2004) *Nat. Struct. Mol. Biol.* **11,** 551–557
45. Nickels, B. E., Mukhopadhyay, J., Garrity, S. J., Ebright, R. H., and Hochschild, A. (2004) *Nat. Struct. Mol. Biol.* **11,** 544–550
46. Mooney, R. A., and Landick, R. (2003) *Genes Dev.* **17,** 2839–2851
47. Borukhov, S., Sagitov, V., Josaitis, C. A., Gourse, R. L., and Goldfarb, A. (1993) *J. Biol. Chem.* **268,** 23477–23482
48. Epshtein, V., Toulmé, F., Rahmouni, A. R., Borukhov, S., and Nudler, E. (2003) *EMBO J.* **22,** 4719–4727